

## Supplemental data and methods

### **D1-mGlu5 heteromers mediate non-canonical dopamine signaling in Parkinson's disease.**

Irene Sebastianutto<sup>§1</sup>, Elise Goyet<sup>§2</sup>, Laura Andreoli<sup>+1</sup>, Joan Font-Ingles<sup>+2</sup>, David Moreno-Delgado<sup>+2,5</sup>, Nathalie Bouquier<sup>2</sup>, Céline Jahannault-Talignani<sup>2</sup>, Enora Moutin<sup>2</sup>, Luisa Di Menna<sup>3</sup>, Natallia Maslava<sup>1</sup>, Jean-Philippe Pin<sup>2</sup>, Laurent Fagni<sup>2</sup>, Ferdinando Nicoletti<sup>3,4</sup>, Fabrice Ango<sup>2</sup>, M. Angela Cenci<sup>\*1</sup>, and Julie Perroy<sup>\*2</sup>

<sup>1</sup> Basal ganglia pathophysiology unit, Dept. Experimental Medical Science, Lund University, Lund, Sweden.

<sup>2</sup> IGF, Univ. Montpellier, CNRS, INSERM, Montpellier, France.

<sup>3</sup> I.R.C.C.S. Neuromed, Pozzilli, Italy.

<sup>4</sup>Dept. Physiology and Pharmacology, Sapienza University of Rome, Italy.

<sup>5</sup> Department of Neuroscience Research, UCB Pharma, Braine l'Alleud, Belgium.

<sup>§</sup> Shared first authors

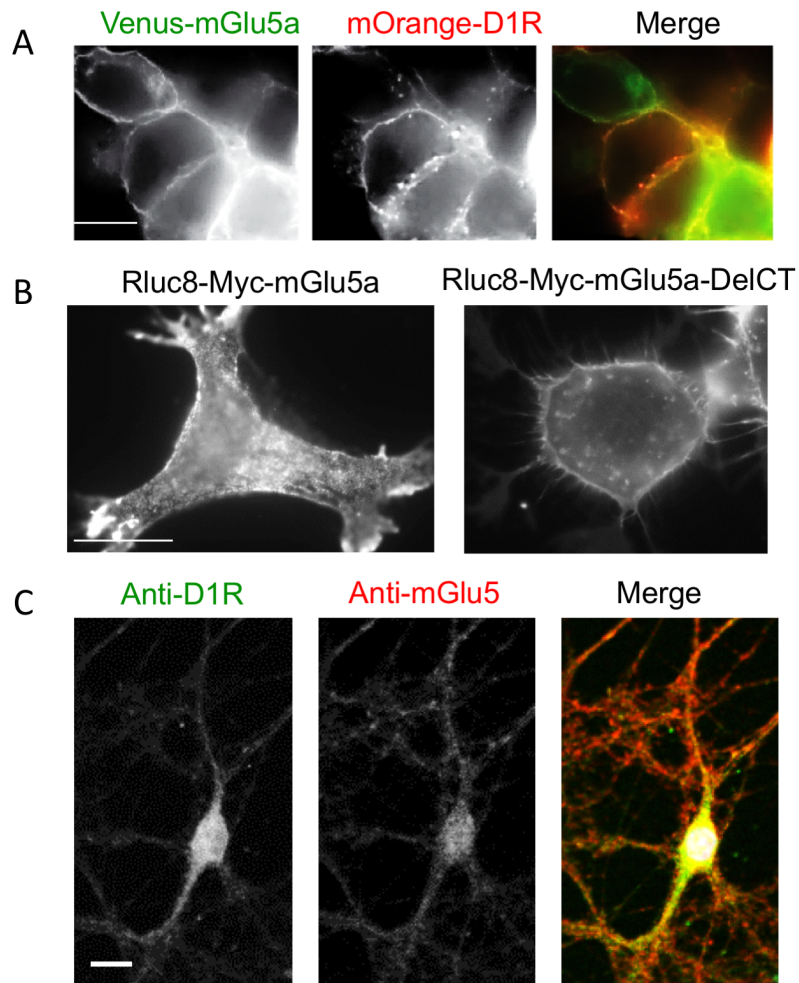
<sup>+</sup> Shared second authors

<sup>\*</sup> Shared senior and corresponding authors

M. Angela Cenci, [Angela.Cenci\\_Nilsson@med.lu.se](mailto:Angela.Cenci_Nilsson@med.lu.se)

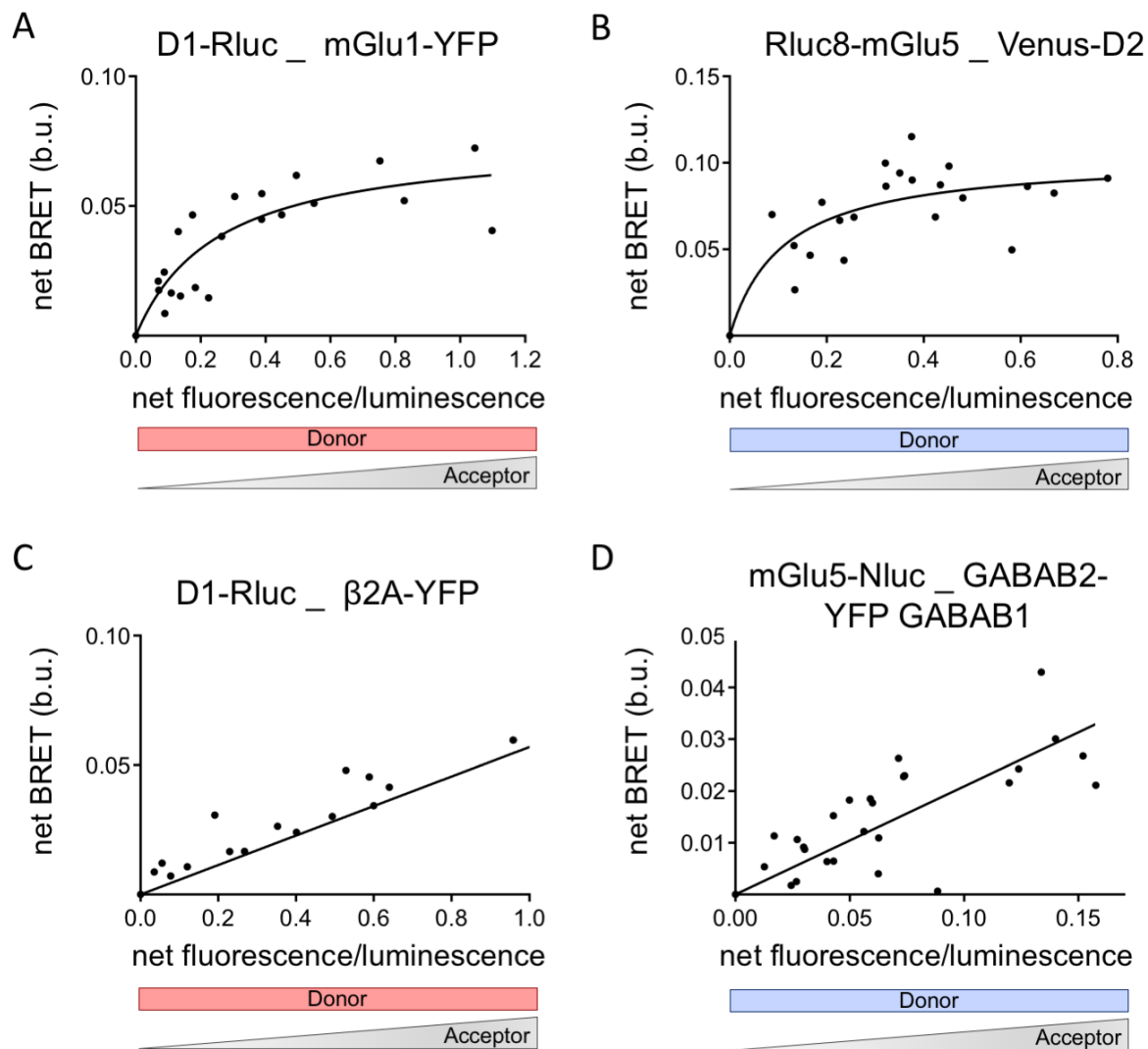
Julie Perroy, [Julie.perroy@igf.cnrs.fr](mailto:Julie.perroy@igf.cnrs.fr)

## Supplemental Figures



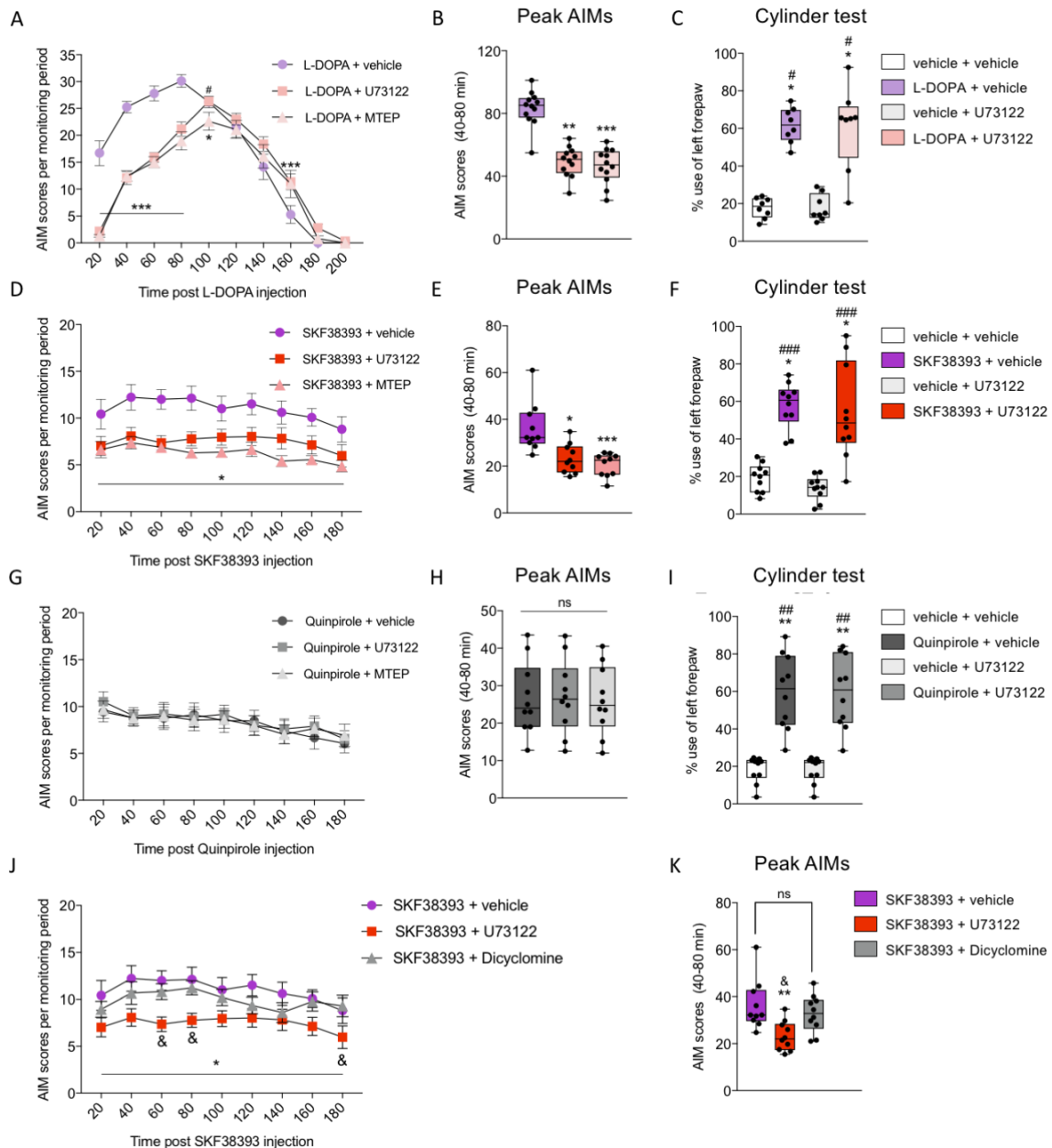
### Suppl. Figure S1 – Receptors expression

**A:** Cell surface fluorescence of Venus-mGlu5 and mOrange-D1 receptors. HEK293 cells were transiently transfected with Venus-mGlu5 and mOrange-D1 receptors coding plasmids. Scale bar 10  $\mu\text{m}$ . **B:** Rluc8-mGlu5DelICT fusion is correctly expressed at the cell surface. HEK293 cells were transiently transfected with Rluc8-Myc-mGlu5 and Rluc8-Myc-mGlu5-DelICT coding plasmids. Surface immunofluorescence was performed using an anti-Myc antibody on fixed but not permeabilized HEK cells. Scale bar 10  $\mu\text{m}$ . **C:** Endogenous D1 and mGlu5 receptors are expressed in primary cultured hippocampal neurons. Immunofluorescence was performed using anti-D1 and anti-mGlu5 antibodies on fixed and permeabilized hippocampal neurons at DIV12. Scale bar 10  $\mu\text{m}$ .



**Suppl. Figure S2 - Characterization of other possible heteromerization partners for D1 or mGlu5 receptors in living cells.** BRET titration curves were measured on HEK293 cells co-transfected with the following receptor constructs: **(A)** D1-Rluc and mGlu1-YFP; **(B)** Rluc8-mGlu5 and Venus-D2; **(C)** D1-Rluc and  $\beta$ 2Ad-YFP; **(D)** mGlu5-Nluc, GABAb1 and GABAb2-YFP. BRET signals were measured for increasing expression levels of acceptor at constant level of donor expression. Results were analyzed by nonlinear regression on a pooled data set from three independent experiments, assuming a model with one-site binding (GraphPad Prism 7). Hyperbolic increases in BRET signal reveal physical receptor interactions, while linear increases report non-specific interactions (most likely reflecting random collision between the receptor constructs).

For a constant expression of D1-Rluc receptor, the BRET signal increased hyperbolically as a function of mGlu1-YFP expression level, reporting a specific interaction between D1 and the mGlu1 receptor, which is quite similar to mGlu5 regarding molecular structure and signal transduction properties (1). Using the same method, mGlu5 was found able to form heteromers with the D2 receptor (panel B). By opposition, we found no specific BRET signal between D1 and  $\beta$ 2 adrenergic receptors, nor between mGlu5 and GABA $\beta$  receptors (see the linear increase in BRET signal, panels C and D), despite previous demonstrations of functional signaling interactions between these receptor categories in different neuronal systems (2-5)).



**Suppl. Figure S3 – Profile of motor effects produced by MTEP and U73122 in dyskinetic rats.**

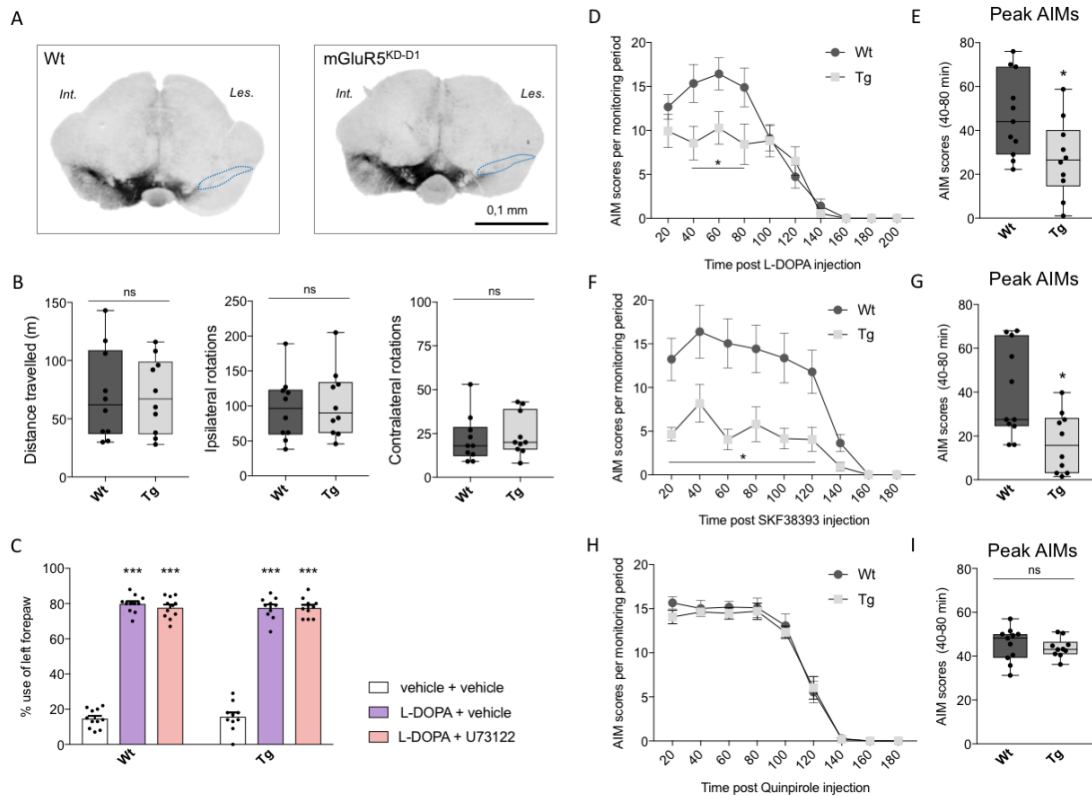
**A-B:** L-DOPA-induced AIMs. **(A)** Time course of AIM scores shows improvement of AIMs between 20-80 min with both treatments ( $n = 12$ ; RM Two-way ANOVA, Treatment:  $F(2,22) = 40.92$ ,  $p < 0.001$ ; Time:  $F(9,99) = 115.5$ ,  $p < 0.001$ ; Interaction:  $F(18,198) = 22.97$ ,  $p < 0.001$ ). **(B)** Peak AIMs ( $n = 12$ ; Friedman test ( $Fr$ ) = 18.17,  $p < 0.001$ ). **(C)** The lesion-induced forelimb use asymmetry is similarly reversed by L-DOPA whether coadministered with U73122 or its vehicle ( $n = 8$ ;  $Fr = 17.46$ ,  $p < 0.001$ ).

**D-E:** SKF38393-induced AIMs. **(D)** Time course of AIM scores shows a significant antidyskinetic effect by MTEP and U73122 throughout the test session ( $n = 10$ ; RM Two-way ANOVA, Treatment:  $F(2,18) = 18.49$ ,  $p < 0.001$ ; Time:  $F(8,72) = 3.67$ ,  $p < 0.01$ ; Interaction:  $F(16,144) = 0.39$ ,  $p = 0.98$ ). **(E)** Peak AIMs ( $n = 10$ ;  $Fr = 15.8$ ,  $p < 0.001$ ). **(F)** The lesion-induced forelimb use asymmetry is similarly reversed by SKF38393 whether coadministered with U73122 or its vehicle ( $n = 10$ ;  $Fr = 25.2$ ,  $p < 0.001$ ).

**G-H:** Quinpirole-induced AIMs. **(G)** Time course of AIM scores shows no significant effect by MTEP or U73122 ( $n = 10$ ; RM Two-way ANOVA, Treatment:  $F(2,18) = 3.86$ ,  $p < 0.05$ ; Time:  $F(8,72) = 4.94$ ,  $p <$

0.001; Interaction:  $F(16,144) = 1.20$ ,  $p = 0.28$ ). **(H)** Peak AIMs ( $n = 10$ ;  $Fr = 1.72$ ,  $p > 0.05$ ). **(I)** The lesion-induced forelimb use asymmetry is similarly reversed by Quinpirole whether coadministered with U73122 or its vehicle ( $n = 10$ ;  $Fr = 26.67$ ,  $p < 0.001$ ).

**J-K:** The muscarinic receptor antagonist dicyclomine does not improve D1 receptor-mediated AIMs. **(J)** Time course of SKF38393-induced AIM scores shows no effect by dicyclomine, while U73122 has a significant antidyskinetic effect in the same animals ( $n = 10$ ; RM Two-way ANOVA, Treatment:  $F(2,18) = 11.65$ ,  $p < 0.001$ ; Time:  $F(8,72) = 3.29$ ,  $p < 0.01$ ; Interaction:  $F(16,144) = 0.56$ ,  $p > 0.05$ ). **(K)** Peak AIMs ( $n=10$ ;  $Fr = 14.21$ ,  $p < 0.001$ ). Symbols of statistical significance refer to post hoc pairwise comparisons carried out with Bonferroni's test (RM ANOVA) or Dunn's test (Friedman test); for panels A-B, D-E, J-K: \* $p < 0.05$ , \*\* $p < 0.01$  and \*\*\* $p < 0.001$  vs. DA receptor agonist + vehicle, respectively; # $p < 0.05$  vs. L-DOPA + MTEP; & $p < 0.05$  vs. SKF38393 + Dicyclomine; for panels C, F, I: \* $p < 0.05$  and \*\* $p < 0.01$  vs. vehicle + vehicle, respectively; # $p < 0.05$ , ##  $p < 0.01$  and ###  $p < 0.001$  vs. vehicle + U73122.



**Suppl. Figure S4 – Behavioural pharmacological studies in transgenic mGluR5<sup>KD-D1</sup> mice.**

**A:** Overview of midbrain sections immunostained for tyrosine hydroxylase (TH) reveal complete loss of dopaminergic neurons in substantia nigra pars compacta (enclosed by blue dotted lines) in both Wt and mGluR5<sup>KD-D1</sup> mice following 6-OHDA lesion (scale bar 0.1 mm). **B:** Spontaneous motor activity in an open field measured from 6-OHDA lesioned Wt (n = 10) and mGluR5<sup>KD-D1</sup> mice (n = 10). Lesioned mice from either genotype displayed comparable levels of total distance travelled (p = 0.98; Mann-Whitney test). In addition, the two genotypes exhibited similar numbers of ipsilateral and contralateral rotations (p = 0.67 and p = 0.49, respectively, Mann-Whitney test). **C:** The cylinder test reveals similar deficits in contralateral forelimb use in 6-OHDA-lesioned Wt mice (n = 11; vehicle + vehicle) and mGluR5<sup>KD-D1</sup> mice (n = 10; vehicle + vehicle). In addition, both genotypes display a similar motor improvement (increase percentage use of contralateral forepaw) after treatment with L-DOPA (see L-DOPA + vehicle). This improvement is not diminished by inhibiting PLC (cf. L-DOPA + U73122 vs. L-DOPA + vehicle). Two-way ANOVA, Treatment: F(2,38)= 779, p < 0.001; Genotype: F(1,19)= 0.08, p = 0.77; Interaction: F(2,38)= 0.43, p = 0.65. Bonferroni's test: \*\*\*p < 0.001 vs. vehicle + vehicle of same genotype. These data exclude a negative impact of either D1 cell-specific mGlu5 knockdown or PLC inhibition on the beneficial anti-akinetic effect of L-DOPA in 6-OHDA-lesioned mice.

**D-E, F-G, H-I:** comparison of AIMs induced by different dopaminergic agents in Wt (n = 11) and transgenic mGluR5<sup>KD-D1</sup> mice (n = 10). **D:** Time course of L-DOPA-induced AIMs shows reduced dyskinesia severity in mGluR5<sup>KD-D1</sup> compared to Wt between 40-80 min (Two-way ANOVA, Genotype: F(1,19)= 2.36, p = 0.14; Time: F(9,171)= 53.77, p < 0.001; Interaction: F(9,171) = 4.21, p < 0.001). **E:** L-DOPA-induced peak AIMs (\*p < 0.05; Mann-Whitney test). **F:** Time course of SKF38393-induced AIMs show a reduced severity of D1 receptor-mediated dyskinesia in mGluR5<sup>KD-D1</sup> compared to Wt animals (Two-way ANOVA, Genotype: F(1,19)= 9.58, p < 0.01; Time: F(8,152)= 25.78, p < 0.001; Interaction: F(8,152)= 5.23, p < 0.001). **G:** SKF38393-induced peak AIMs (\*p < 0.05; Mann-Whitney test). **H:** Time course and severity of quinpirole-induced AIMs do not differ between the two genotypes (Two-way ANOVA, Genotype: F(1,19)= 0.4, p = 0.53; Time: F(8,152)= 220.6, p < 0.001; Interaction: F(8,152)= 0.40, p = 0.93). **I:** Quinpirole-induced peak AIMs (p = 0.61; Mann-Whitney test).

Suppl. Table 1: Drugs, doses and administration procedures used.

Drug	Principle of action	Supplier	Admin. route	Main doses (mg/kg)		Vehicle	AIMs test: Adm. Interval to DA agonist	Main references
				Rat	Mouse			
L-DOPA	DA precursor	Sigma Aldrich	s.c.	6	(3) 6	Saline	0 min	(6, 7)
SKF38393	D1-like agonist	Sigma Aldrich	s.c.	2	(3) 6	Saline	0 min	(8)
Quinpirole	D2 agonist	Sigma Aldrich	s.c.	0.1	(0.1) 0.5	Saline	0 min	(9)
MTEP	mGlu5 antagonist	Abcam	s.c.	5	5	Saline	0 min	(8)
U73122	PLC inhibitor	Tocris Bioscience	s.c.	30	10	5% DMSO + Saline	20 min	(10)
Dicyclo-mine	Muscarinic receptor antagonist	Sigma Aldrich	i.p.	15	-	Saline	30 min	(11)

Suppl. Table 1: Parenthesized are the doses used during AIMs induction phase. References pertain to studies using the compound together with L-DOPA, and refer to dosage and interval of administration between the two drugs.

## **Supplemental Materials and Methods**

**Reagents.** Coelenterazine H, Furimazine and D-luciferin were obtained from Promega. Drugs were purchased from Tocris and used at the following concentrations (except when otherwise indicated): DHPG: (S)-3,5-Dihydroxyphenylglycine (100  $\mu$ M), SKF-81297: ( $\pm$ )-6-Chloro-2,3,4,5-tetrahydro-1-phenyl-1H-3-benzazepine hydrobromide (10  $\mu$ M), MTEP: 3-((2-Methyl-1,3-thiazol-4-yl)ethynyl)pyridine hydrochloride (10  $\mu$ M), L-Quisqualic acid (10  $\mu$ M), LY341495: (2S)-2-Amino-2-[(1S,2S)-2-carboxycycloprop-1-yl]-3-(xanth-9-yl) propanoic acid (100  $\mu$ M).

**Dopamine-denervating lesions.** Mice were anesthetized using a mixture of 4% isoflurane in air (Isobavet, Apoteksbolaget), placed in a stereotaxic frame with a mouse adaptor (Kopf Instruments, Tujunga, USA), and kept anesthetized using 2% isoflurane. The toxin 6-OHDA-HCl (Sigma Aldrich, Stockholm, Sweden) was dissolved in a 0.02% ascorbic acid-saline solution (3.2  $\mu$ g free-base 6-OHDA per  $\mu$ l) and 1  $\mu$ l was injected at the following coordinates (in mm, relative to bregma and dural surface, and with the animal on flat-skull position): AP = -0.7, ML = -1.2, DV = -4.7. The injection was made using a glass capillary, attached to a 10  $\mu$ l Hamilton syringe, at the rate of 0.5  $\mu$ l/min; the capillary was left in place for 2 min before and 2 min after the injection. The analgesic Marcain (bupivacaine, 2.5 mg/ml, AstraZeneca) was injected subcutaneously (10  $\mu$ l/10 g, body weight) before first skin incision. Mouse postoperative care was performed as in (6). Rats were anesthetized with a 20:1 mixture of Fentanyl and Dormitor (Apoteksbolaget, Sweden AB), delivered by i.p. injection, and placed in a stereotaxic frame (Kopf Instruments, Tujunga, USA). The 6-OHDA solution was prepared as for the mouse and injected at the following coordinates (in mm, relative to bregma and dural surface): first injection: AP = -4.4, ML = -1.2, DV = -7.8, tooth bar = +2.4 (2,5  $\mu$ l); second injection: AP = -4.0, ML = -0.8, DV = -8.0, tooth bar = +3.4 (2,0  $\mu$ l). After surgery, animals received analgesic treatment with Temgesic (Apoteksbolaget AB, Sweden).

**Abnormal involuntary movements (AIMs) ratings.** Each animal was rated online for 1 min every 20 min for up to 200 min following the injection of a DAergic agent. Three topographic subtypes of dyskinesia were considered: (i) axial AIMs (twisting of the neck and upper trunk towards the side contralateral to the lesion), (ii) forelimb AIMs (purposeless movements or dystonic posturing of the contralateral forelimb), (iii) orolingual AIMs (facial/jaw movements and contralateral tongue protrusion). These three AIM subtypes were scored simultaneously on two severity scales (each graded from 0 to 4), one based on the proportion of observation time during which dyskinetic movements were present, the other one based on movement amplitude (i.e. degree of deviation of the dyskinetic body part from its natural resting position). Time-based severity scores were multiplied by the



amplitude scores for each AIM subtype and observation point, and the sum of these products was used in the final analysis. The sum of AIM scores between 40 and 80 min after the injection of a DAergic agent was defined as “peak-AIMs” in agreement with previous studies (8, 12, 13).

**Open field activity:** This test was used as a part of the phenotypic characterization of mGluR5<sup>KD-D1</sup> mice after the 6-OHDA lesion (see Suppl. Figure S4). Mice were monitored in an open field using a video-tracking system (Stoelting ANY-MAZE video tracking) that detects the position of the animal’s head, body, and tail in the arena (transparent Plexiglas boxes of 50 x 50cm). The system provides measures of spontaneous horizontal activity (distance travelled) and turning movements (based on the rotation of the mouse body axes) expressed as the number of clockwise and anticlockwise full turns. Each recording session lasted 160 min and data were expressed as total distance travelled (in meters) and total number of ipsi- or contralateral turns.

**Immunohistochemistry.** Coronal striatal sections were incubated for 1 hour in blocking solution (5% normal goat serum, NGS, in Tris-buffered saline (TBS-T: TBS containing 0.1% Triton-X) and were then incubated for 24-48 hours with one of the following primary antibodies: rabbit anti-phospho<sup>Thr202/Tyr204</sup> ERK1/2 (#9101; Cell Signaling Technology, 1:250; rabbit anti-TH (#P40101; Pel-Freeze, Rogers, AR, 1:1000). Sections were then rinsed and incubated with biotinylated goat-anti-rabbit antibodies (BA1000; Vector Laboratories, Burlingame, CA, U.S.A., 1:200 in 2.5% NGS-TBS-T). Following incubation with an avidin-biotin-peroxidase complex (Vectastain Elite ABC-kit; Vector Laboratories, Burlingame, CA, U.S.A.), immunocomplexes were visualized using 3’3’-diaminobenzidine (DAB) and H<sub>2</sub>O<sub>2</sub> (both from Sigma Aldrich, Sweden). Slide-mounted sections were dehydrated and coverslipped with DPX mounting medium (Sigma Aldrich, Sweden). Additional details regarding our methods of tissue preparation and immunohistochemistry can be found in (14).

## Supplemental References

1. Abe T, Sugihara H, Nawa H, Shigemoto R, Mizuno N, and Nakanishi S. Molecular characterization of a novel metabotropic glutamate receptor mGluR5 coupled to inositol phosphate/Ca<sup>2+</sup> signal transduction. *J Biol Chem*. 1992;267(19):13361-8.
2. Lei S. Cross interaction of dopaminergic and adrenergic systems in neural modulation. *Int J Physiol Pathophysiol Pharmacol*. 2014;6(3):137-42.
3. Smith Y, Charara A, Hanson JE, Paquet M, and Levey AI. GABA(B) and group I metabotropic glutamate receptors in the striatopallidal complex in primates. *J Anat*. 2000;196 ( Pt 4):555-76.
4. Gubellini P, Pisani A, Centonze D, Bernardi G, and Calabresi P. Metabotropic glutamate receptors and striatal synaptic plasticity: implications for neurological diseases. *Prog Neurobiol*. 2004;74(5):271-300.
5. Dickerson JW, and Conn PJ. Therapeutic potential of targeting metabotropic glutamate receptors for Parkinson's disease. *Neurodegener Dis Manag*. 2012;2(2):221-32.
6. Sebastianutto I, Maslava N, Hopkins CR, and Cenci MA. Validation of an improved scale for rating L-DOPA-induced dyskinesia in the mouse and effects of specific dopamine receptor antagonists. *Neurobiol Dis*. 2016;96:156-70.
7. Lindgren HS, Rylander D, Ohlin KE, Lundblad M, and Cenci MA. The "motor complication syndrome" in rats with 6-OHDA lesions treated chronically with L-DOPA: relation to dose and route of administration. *Behav Brain Res*. 2007;177(1):150-9.
8. Iderberg H, Rylander D, Bimpisidis Z, and Cenci MA. Modulating mGluR5 and 5-HT1A/1B receptors to treat L-DOPA-induced dyskinesia: effects of combined treatment and possible mechanisms of action. *Exp Neurol*. 2013;250:116-24.
9. Delfino MA, Stefano AV, Ferrario JE, Taravini IR, Murer MG, and Gershanik OS. Behavioral sensitization to different dopamine agonists in a parkinsonian rodent model of drug-induced dyskinesias. *Behav Brain Res*. 2004;152(2):297-306.
10. Medvedev IO, Ramsey AJ, Masoud ST, Bermejo MK, Urs N, Sotnikova TD, et al. D1 dopamine receptor coupling to PLCbeta regulates forward locomotion in mice. *J Neurosci*. 2013;33(46):18125-33.
11. Ding Y, Won L, Britt JP, Lim SA, McGehee DS, and Kang UJ. Enhanced striatal cholinergic neuronal activity mediates L-DOPA-induced dyskinesia in parkinsonian mice. *Proc Natl Acad Sci U S A*. 2011;108(2):840-5.
12. Rylander D, Iderberg H, Li Q, Dekundy A, Zhang J, Li H, et al. A mGluR5 antagonist under clinical development improves L-DOPA-induced dyskinesia in parkinsonian rats and monkeys. *Neurobiol Dis*. 2010;39(3):352-61.
13. Breger LS, Dunnett SB, and Lane EL. Comparison of rating scales used to evaluate L-DOPA-induced dyskinesia in the 6-OHDA lesioned rat. *Neurobiol Dis*. 2013;50:142-50.
14. Westin JE, Vercammen L, Strome EM, Konradi C, and Cenci MA. Spatiotemporal pattern of striatal ERK1/2 phosphorylation in a rat model of L-DOPA-induced dyskinesia and the role of dopamine D1 receptors. *Biol Psychiatry*. 2007;62(7):800-10.